Cooperative Recombination of a Quantized High-Density Electron-Hole Plasma in Semiconductor Quantum Wells

Y. D. Jho,[1,3] Xiaoming Wang,[1] J. Kono,[2] D. H. Reitze,[1] X. Wei,[3] A. A. Belyanin,[4] V. V. Kocharovsky,[4,5] Vl. V. Kocharovsky,[5] and G. S. Solomon[6]

[1]*Department of Physics, University of Florida, Gainesville, Florida 32611, USA*
[2]*Department of Electrical and Computer Engineering, Rice University, Houston, Texas 77005, USA*
[3]*National High Magnetic Field Laboratory, Florida State University, Tallahassee, Florida 32310, USA*
[4]*Department of Physics, Texas A&M University, College Station, Texas 77843, USA*
[5]*Institute of Applied Physics, Russian Academy of Sciences, 603950 Nizhny Novgorod, Russia*
[6]*Solid-State Laboratories, Stanford University, Stanford, California 94305, USA*
(Received 21 December 2005; published 12 June 2006)

We investigate photoluminescence from a high-density electron-hole plasma in semiconductor quantum wells created via intense femtosecond excitation in a strong perpendicular magnetic field, a fully quantized and tunable system. At a critical magnetic field strength and excitation fluence, we observe a clear transition in the band-edge photoluminescence from omnidirectional output to a randomly directed but highly collimated beam. In addition, changes in the linewidth, carrier density, and magnetic field scaling of the photoluminescence spectral features correlate precisely with the onset of random directionality, indicative of cooperative recombination from a high-density population of free carriers in a semiconductor environment.

PACS numbers: 78.67.De, 78.20.Ls, 78.55.−m

The spontaneous appearance of macroscopic coherence is among the most dramatic cooperative phenomena in condensed matter physics. Superconductivity [1] is the most prominent example, and solid-state analogs of Bose-Einstein condensation are actively being pursued [2]. A related fundamental cooperative process exists in quantum optics, superfluorescence (SF) [3–5], in which an incoherently prepared system of N inverted atoms develops macroscopic coherence self-consistently from vacuum fluctuations. The resultant macroscopic dipole decays superradiantly [6,7], producing a burst of coherent radiation. Superfluorescence has been observed in atomic gases [8,9] and rarefied impurities in crystals [10–12].

The observation of cooperative recombination in semiconducting systems is significantly more challenging due to ultrafast decoherence. Nevertheless, investigations of such phenomena, especially in strong magnetic fields, are important because they allow us to probe quantum coherence in a previously inaccessible regime. Coherent carrier dynamics in semiconductors has received much attention in recent years owing to the development of ultrafast lasers, but most of these investigations have focused on excitons at relatively low densities [13]. Probing SF emission in semiconductors provides insight into the cooperative behavior of dense electron-hole (*e-h*) plasmas in quantum-engineered semiconductors. Potentially, they can lead to novel sources of intense, tunable, and ultrashort pulses in the near and midinfrared regions and possibly establish new routes to controlling electronic interactions at high densities using strong magnetic fields.

Pure SF [3,4] is characterized by several signatures that uniquely distinguish it from other emission processes. A

SF pulse is bright, highly collimated, and of short duration (less than the homogeneous dephasing time T_2). SF is inherently random: polarization fluctuations grow from initially incoherent quantum noise and reach a macroscopic level. Thus, the emission direction varies from shot to shot. In addition, a SF pulse appears after a delay time during which mutual coherence between individual dipoles is established. Note the principal difference between SF and superradiance [6,7,14,15]: the latter develops in a system in which the macroscopic polarization has been initially established by an external laser field. The key parameter governing the growth rate of cooperative emission is the coupling strength between the electromagnetic field and optical polarization, expressible as the cooperative frequency, ω_c [4,16]. To observe SF from a system of *e-h* pairs in a semiconductor quantum well (QW),

$$\omega_c = \sqrt{\frac{8\pi^2 d^2 N \Gamma c}{\hbar n^2 \lambda L_{\text{QW}}}} \qquad (1)$$

must exceed $2/T_2$ [or $2/(T_2 T_2^*)^{1/2}$ if the inhomogeneous dephasing time $T_2^* < T_2$]. Here d is the transition dipole moment; N, 2D *e-h* density; Γ, overlap of radiation with the QWs; $\hbar$, Planck's constant; n, refractive index; λ, wavelength (in vacuum); c, speed of light; and L_{QW}, total width of the QWs. Under the optimal SF conditions, the pulse duration scales as $\tau_{\text{SF}} \sim 1/\omega_c \sim N^{-1/2}$ and thus the peak intensity scales as $I_{\text{SF}} \sim \hbar \omega N / \tau_{\text{SF}} \sim N^{3/2} \sim B^{3/2}$, where B is a magnetic field applied perpendicular to the QW[4,16]; see also Sec. XII in [5].

Here, we investigate light emission in an undoped QW system in a strong perpendicular magnetic field. The field

fully quantizes the QW system into an atomiclike system with a series of Landau levels (LLs) and thus strongly increases the density of states (DOS) to accommodate a high-density e-h plasma. We measure emission as a function of laser fluence (F_{laser}) and B. The emission characteristics depend upon N ($\sim F_{laser}$) and B, evolving from omnidirectional, inhomogeneously broadened photoluminescence (PL) at low densities and fields through a narrowly peaked but omnidirectional output $\sim N$ to a randomly directed but highly collimated output $\sim N^{3/2} \sim B^{3/2}$ as the field increases. The successive stages of emission progress from low-density PL through a regime where amplified spontaneous emission (ASE) dominates into a regime characterized by stochastically oriented but highly directional emission.

Samples were grown by molecular-beam epitaxy on GaAs, consisting of a GaAs buffer followed by 15 layers of 8-nm $In_{0.2}Ga_{0.8}As$ QWs separated by 15-nm GaAs barriers and a 10-nm GaAs cap layer. Their PL and absorption spectra at high magnetic fields are thoroughly described in Ref. [17]. We used a 150 fs, 775 nm Ti:sapphire regenerative amplifier system, and measured the PL as a function of F_{laser}, B, and pump spot size and geometry, up to 9.7 mJ/cm^2, 28 T, and 3×3 mm^2 (the sample size), respectively. Approximately $10^{12} e$-h pairs/cm^2 were generated for $F_{laser} \sim$ 0.01 mJ/cm^2. The laser beam was delivered into a 31 T Bitter-type magnet through free space and focused using a spherical or cylindrical lens. The QW plane was perpendicular to B. Emission was collected using optical fibers from the opposite face and cleaved edges of the sample and analyzed with a grating spectrometer equipped with a charge-coupled device detector. Unless noted, each spectrum consisted of the emission from ~1000 pulses. Two right angle microprisms redirected the edge emission from the sample to collection fibers. The collection area of the prisms was 1×1 mm^2, and the computed acceptance angle based on geometry was ~40°. Excitation at 775 nm creates carriers high in the bands with an excess energy of 270 meV (the energy difference between the initial carrier states and the 0-0 LL [18]), and thus a very short T_2 (a few fs). The carriers then thermalize, becoming quantized with a longer T_2. Thus, the resulting e-h plasma is initially completely incoherent.

Figure 1 shows spectra collected at the sample edge perpendicular to the excitation direction, i.e., emission in the QW plane (a) versus B at a fixed F_{laser} and (b) versus F_{laser} at a fixed B (20 T) at 10 K for an excitation spot size of 0.5 mm. A threshold is observed in both cases; inhomogeneously broadened PL peaks (~9 meV) are seen at each interband LL transition until F_{laser} and B exceed a threshold value, whereupon a narrow peak (~2 meV) emerges from the high-energy side of the broad feature and dominates at high F_{laser}. Identical spectra are seen when collecting from above the pump spot, i.e., out of plane (left inset), although at a much lower efficiency. Increasing or decreas-
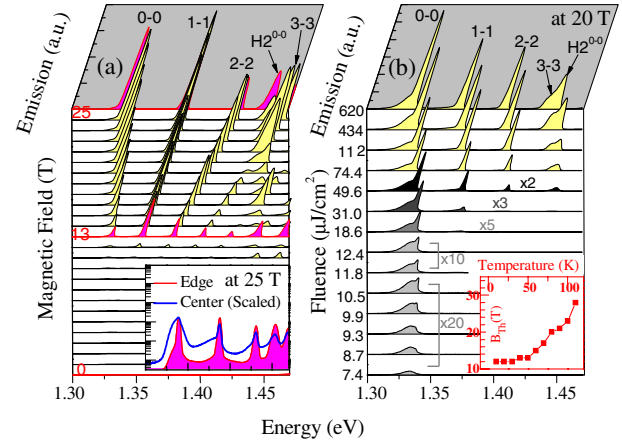

FIG. 1 (color online). Emission spectra as a function of (a) magnetic field for fixed fluence (0.62 mJ/cm^2) and (b) fluence for a fixed field (20 T). To compare the edge (red line) to center (blue line) collection in the inset of Fig. 1(a), the opposite face is multiplied by 5000. The inset in (b) shows how the threshold magnetic field depends on temperature.

ing the pump spot size resulted in the emergence of sharp PL features in the spectra at a given fluence. Thus, the observed behavior is not due to a spatially or spectrally inhomogeneous distribution of carriers. Sharp emission features are observed to 130 K (right inset), with the threshold field for 0-0 LL increasing from 12 to 28 T as the temperature increases from 10 to 110 K.

The integrated strength of the 0-0 LL emission versus B [Fig. 2(a)] and F_{laser} [Fig. 2(b)] was obtained from a Lorentzian line shape analysis of the narrow blueshifted feature for a 0.5 mm excitation spot. Below 12 T (and 0.01 mJ/cm^2), narrow emission is not observed. In the range 12–14 T (0.01–0.03 mJ/cm^2), the signal grows linearly (green lines) with both B and F_{laser}. Above 14 T (0.03 mJ/cm^2), the emission strength becomes superlinear (blue lines) with the integrated signal $S \propto B^{3/2}$. Above 0.2 mJ/cm^2 in Fig. 2(b), the signal resumes a linear scaling. The linewidths (red circles), also plotted in Figs. 2(a) and 2(b) reveal a remarkable correlation with the emission strength. In the linear regime, the linewidth decreases monotonically both versus B and F_{laser} until the emission becomes superlinear, where the linewidth begins to *increase*. When the laser spot was increased (decreased) to 3 mm (0.1 mm) as shown in Figs. 2(c) and 2(d), narrow emission was observed, but both the integrated signal S and the linewidth exhibited qualitatively different scaling, and in both of these cases, the linewidth monotonically decreased with increasing fluence.

Figure 3 presents the directionality of the emission for single pulse excitation. Figure 3(b) illustrates a series of spectra upon *single* pulse excitation at a fluence corresponding to the superlinear emission regime in Fig. 1 (9.7 mJ/cm^2, 25 T) for a 0.5 mm diameter spot size collected through edge 1 (black) and edge 2 (red). Figure 3(c) displays the maximum peak height from each
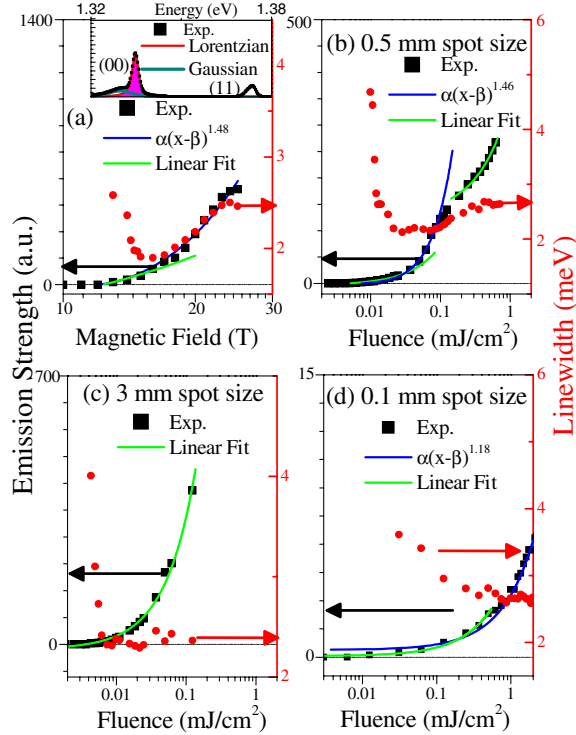
FIG. 2 (color online). Emission strength and linewidth of the narrow peak from the 0-0 LL versus (a) B and (b),(c),(d) F_{laser} for different pump spot sizes. Both B and F_{laser} are on a logarithmic scale. The inset of (a) shows the convolution method using a Lorentzian for the sharp peak and a Gaussian for the broader lower-energy peak. The blue (green) lines in (a)–(d) indicate the superlinear (linear) regime.
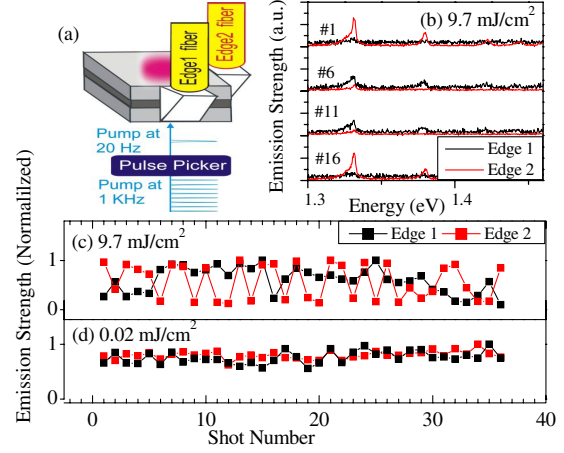

FIG. 3 (color online). (a) Experimental schematic showing single-shot excitation and collection. (b) Four representative emission spectra from edge 1 (black) and edge 2 (red) fibers, excited from single laser pulse and measured simultaneously. Normalized emission strength from the 0th LL versus shot number in the (c) SF regime and (d) ASE regime.

edge (normalized to 1.0) versus shot number for the pumping conditions in Fig. 3(b). The maximum observed emission strength in Fig. 3(c) fluctuates as much as 8 times the minimum value, far greater than the pump pulse fluctuation (~2%). This strong anticorrelation between signals received by different edges indicates a collimated but randomly changing emission direction from pulse to pulse. At a lower $F_{laser} = 0.02$ mJ/cm^2 (obtained with a 3 mm spot), qualitatively different behavior is seen; Fig. 3(d) shows omnidirectional emission on every shot, as expected for ASE or PL. We also probed the spatial and directional characteristics of the emission process. Using a cylindrical lens to generate a rodlike excitation region, we measured the signal as a function of angle from 0° to 180° for $F_{laser} = 0.02$ mJ/cm^2 and $B = 25$ T (not shown). The emission was highly directional with a 40° divergence, comparable to the measurement acceptance angle. In addition, the measured amplitude ratio along the long axis relative to the short axis was consistent with exponential gain, as expected for a stimulated process.

The scaling of the LL peaks, the linewidth evolution, and emission directionality point to the following evolution as F_{laser} and B are increased: (i) In the low-density limit ($B < 12$ T, $F_{laser} < 5$ μJ/cm^2), excited e-h pairs relax and radiate spontaneously through interband recom-

bination. The emission is isotropic with an inhomogeneous Gaussian width of ~9 meV. (ii) At a critical fluence ~0.01 mJ/cm^2 and $B = 12$ T, population inversion is established and ASE develops, leading to the emission of pulses. Figure 3(d) shows that ASE is simultaneously emitted in all directions in the plane. The reduction in linewidth with increasing fluence results from conventional gain narrowing: spectral components near the maximum of the gain spectrum are preferentially amplified than components with greater detuning [Figs. 2(a) and 2(b) below 17 T and 0.03 mJ/cm^2]. In the high-gain regime, the spectral width reduces to 2 meV FWHM but is still larger than $2/T_2$. (iii) When the DOS and physical density are sufficiently high, the cooperative frequency ω_c [Eq. (1)] exceeds $2/(T_2 T_2^*)^{1/2}$. The e-h pairs establish a macroscopic dipole after a short delay time and emit a pulse through cooperative recombination (or a sequence of pulses, depending on the pump fluence and the size of the pumped area). Because of inhomogeneous broadening, the pulse spectral width (inverse duration) can be smaller than the total width of the radiation, so there is no strong broadening of the line, as shown in Fig. 2(a). Only at very high pump powers the line broadens due to the reduced pulse duration, until eventually saturation (due to the filling of all available states) halts the further decrease in pulse duration. The transition from ASE to cooperative emission at 0.03 mJ/cm^2 is consistent with this observation. Significantly, we find that unlike ASE, which should be emitted in all directions with the same intensity [Fig. 3(d)], in this regime the initial quantum fluctuations grow to a macroscopic level to establish coherence and lead to strong directional fluctuations from shot to shot [Fig. 3(c)]. The return to linear scaling above 0.1 mJ/cm^2 is a combined result of absorption saturation of the pump and saturation of SF emission.

Since the data was collected in a time-integrated fashion, we cannot directly probe the peak SF intensity scaling mentioned after Eq. (1). There are two lines of evidence indicating that the observed superlinear scaling is due to the formation of *multiple* SF pulses from the 0-0 LL. The superlinear increase for the 0-0 emission is accompanied by an emission decrease from higher LLs, implying a fast depletion of the 0-0 level through SF followed by a rapid relaxation of *e-h* pairs from higher LLs and subsequent reemission. Also, the single pulse data shows that the two fiber outputs are either correlated or anticorrelated in roughly equal proportion. Fast relaxation from higher LLs replenishes the 0-0 LL, resulting in a second pulse of SF emission in a random direction. On average, in 50% shots both edges receive a SF pulse, and in the other 50% shots, only one edge will receive both pulses, in qualitative agreement with observations.

It could be argued that the observed emission characteristics are consistent with pure ASE ("lasing"), but this can be ruled out as follows. Collimated, randomly directed emission, and superlinear scaling are observed *only* when the pumped spot is 0.5 mm, approximately equal to the theoretically predicted coherence length for SF emission in QWs, $L_c \sim c\tau_{SF} \ln(I_{SF}/I_{SE})$. They are not observed for 0.1 and 3 mm spot sizes. Furthermore, feedback from facet reflection is naturally suppressed in our structures: propagation modeling indicates that the emission is guided in the pumped region due to polariton dispersion. Optically excited *e-h* pairs create a Lorentzian-type dispersion of the refractive index $n \sim N\Delta/(\Delta^2 + \gamma^2)$ near the central frequency of each interband LL transition, where Δ is the detuning from the transition frequency and γ is the linewidth. The enhancement of n on the high-energy side of the inverted interband LL transition in the pumped region, added to the background index contrast between the MQW and substrate, is able to support guided modes confined only in the pumped region. Such modes will be blueshifted by $\Delta \sim \gamma$ with respect to the peak of the spontaneous PL line, in agreement with Fig. 1. Once the radiation leaves the pumped region, it diverges such that $\sim 5 \times 10^{-4}$ gets coupled back into the guided mode. Self-guiding in the pumped region is essential for achieving high-gain ASE and then SF. Additional suppression comes from the area outside the pump region, since it acts as a high loss absorber comprised of an ensemble of two-level systems in the ground state. Finally, pure SF does not require a rodlike geometry. As shown in Refs. [4,19], cooperative recombination is not constrained by the geometry of the excitation region. Omnidirectional superfluorescent emission has been observed in cesium [19]. Moreover, the disklike geometry of the pumped active region allows us to observe the key evidence for SF, namely, strong shot-to-shot fluctuations in the emission direction. Previous experiments almost exclusively employed a rodlike geometry, in which the only direct signature of SF is the macroscopic fluctua-

tions of the delay time of the SF pulse. In a semiconductor system they would be manifested on the sub-ps scale and very hard to observe.

In conclusion, we have observed cooperative emission in a highly photoexcited, strongly coupled semiconductor system. Using intense ultrafast excitation and strong magnetic fields, the resulting density and energy confinement is sufficient to generate a spontaneous macroscopic polarization that decays through the emission of SF pulses. Our experiments observe this phenomenon by exploiting its quantum-stochastic nature and demonstrate that photon-mediated quantum coherence can develop spontaneously even in strongly interacting semiconductor systems.

[1] See, e.g., P. G. de Gennes, *Superconductivity of Metals and Alloys* (Benjamin, New York, 1966).

[2] See, e.g., H. Deng, G. Weihs, C. Santori, J. Bloch, and Y. Yamamoto, Science **298**, 199 (2002); L. V. Butov, J. Phys. Condens. Matter **16**, R1577 (2004); J. P. Eisenstein and A. H. MacDonald, Nature (London) **432**, 691 (2004).

[3] See, e.g., A. E. Siegman, *Lasers* (University Science Books, Sausalito, 1986), p. 549.

[4] V. V. Zheleznyakov, V. V. Kocharovsky, and Vl. V. Kocharovsky, Sov. Phys. Usp. **32**, 835 (1989).

[5] R. Bonifacio and L. A. Luiato, Phys. Rev. A **11**, 1507 (1975).

[6] R. H. Dicke, Phys. Rev. **93**, 99 (1954).

[7] N. E. Rehler and J. H. Eberly, Phys. Rev. A **3**, 1735 (1971).

[8] N. Skribanowitz *et al.*, Phys. Rev. Lett. **30**, 309 (1973).

[9] H. M. Gibbs *et al.*, Phys. Rev. Lett. **39**, 547 (1977).

[10] R. Florian *et al.*, Solid State Commun. **42**, 55 (1982).

[11] P. V. Zinoviev *et al.*, Sov. Phys. JETP **58**, 1129 (1983).

[12] M. S. Malcuit *et al.*, Phys. Rev. Lett. **59**, 1189 (1987).

[13] See, e.g., J. Shah, *Ultrafast Spectroscopy of Semiconductors and Semiconductor Nanostructures* (Springer-Verlag, Berlin, 1999).

[14] T. Tokihiro *et al.*, Phys. Rev. B **47**, 2019 (1993).

[15] G. Björk *et al.*, Phys. Rev. B **50**, 17 336 (1994).

[16] A. A. Belyanin *et al.*, Quantum Semiclass. Opt. **9**, 1 (1997); Quantum Semiclass. Opt. **10**, L13 (1998); Laser Phys. **13**, 161 (2003).

[17] Y. D. Jho *et al.*, Phys. Rev. B **72**, 045340 (2005).

[18] The high-field Landau notation is used here. For low-field–high-field correspondence, see, e.g., A. H. MacDonald and D. S. Ritchie, Phys. Rev. B **33**, 8336 (1986).

[19] A. I. Lvovsky *et al.*, Phys. Rev. Lett. **82**, 4420 (1999).